MorphCT Results - Device Simulations

Matthew Jones

September 7, 2017

1 Test System

NOTE: We still don't have a real device morphology to work with, so I've bodged one together from the data we already have. It will not suffice for publication, but I'm hoping it will allow me to get all the moving parts in place before we set the code loose on a physical system

```
# Z = 9 + 1 ANODE
1 1 1 0 0 0 0 0 0
0 1 1 1 0 0 0 0 0
0 0 1 1 1 1 0 0 0
0 1 1 1 0 0 0 0 0
2 2 2 2 2 2 2 2 2
3 3 3 4 3 3 3 3 3
3 3 3 4 4 4 3 3 3
3 3 3 3 4 4 3 3 3
3 3 3 3 4 4 4 3 3
# Z = 0 - 1 CATHODE
```

Figure 1: A single slice of the test device used to write and configure the device-scale KMC code

ID	Simulation Name	XML Name	$l_{x,y,z}$ (Å)
0	orderedP3HT	p1-L15-f0.0-P0.1-T1.5-e0.5	85.19
1	disorderedP3HT	shrunkp1-L15-f0.0-P0.1-T2.0-e0.5	85.19
2	interfaceP3HTC60	p1-L15-f0.3-P0.1-T1.5-e0.1	96.23
3	disorderedPCBM	pcbm-0.5-P0.5-300-T3.0_AA	65.69
4	orderedPCBM	pcbm-0.5-P1.5-200-T5.0_AA	57.53

Table 1: The morphologies selected for use in each cell in the device. The ID integers correspond to 'moietyType', and '$l_{x,y,z}$' is the cubic box length for each molecular system.

- The device is a cube consisting of 9x9x9 Cartesian lattice of 'cells' or 'moieties', where each cell in the lattice corresponds to one $\sim$ 10 nm molecular morphology.

- The layout of a single x-z slice of the device is depicted in figure 1. Each cell is assigned an integer [0-4], which represents the molecular morphology type within as described in table 2.4. The structure is therefore a simple bilayer, with regions of crystalline donor and acceptor material in amongst the amorphous melt.

- 9 identical copies of the slice are combined in the y-direction to make the 3D structure.

- Note that the molecular morphology describing each of these cells is actually a different size. On average, each cell represents a structure that is cubic with side 7.8 nm, and so this value was used when calculating displacements within the device.

- Additionally, no orientational manipulation has been applied to these systems. That is, that all of the P3HT crystal cells in the system are identical and oriented the same way. Similarly, the interface cells (which form vertical lamellae of P3HT in the middle and C60 molecules aggregating around the outside) have not been rotated or manipulated in any way.

- The device is periodic in the x and y directions, but is capped at $Z = -1$ and $Z = 9$ by planes that describe the cathode and anode respectively. Carriers crossing into these planes are counted towards the generated photocurrent, and excitons are forbidden from hopping into them. Eventually, these planes will also consider dark-current injection which is vital for device operation.

2 Getting Excitons Working

Before including carrier hopping (which will require a calculation and treatment of coulombic and field effects etc.), it is important to get the exciton dynamics correct.

- Excitons are injected into the device according to the photoinjection rate:

$$k_{\text{photo}} = \Phi \frac{\lambda}{hc} A \left(1 - \exp^{-\alpha(z)}\right), \tag{1}$$

  where Φ is the incident flux (0.01 mW/cm^2), λ is the wavelength (500 nm), A is the photosensitive area (9 $\times$ 7.8 nm $\times$ 9 $\times$ 7.8 nm), and α is the thickness-dependent absorption coefficient (1.3×10^4 $\times$ 9 $\times$ 7.8 $\times10^{-9}$)

- This rate is converted to a wait time for the next photoinjection using the normal KMC algorithm, and then an exciton is placed in a random cell, on a random chromophore after the wait time.

- Only after the exciton has been injected is the next photoinjection wait time calculated.

- The exciton is then permitted to hop based on a modified Förster hopping rate:

$$k_{\text{FRET}} = \frac{B}{\tau_{\text{ex}}} \left(\frac{r_F}{r_{ij}}\right)^6, \tag{2}$$

  where τ_{ex} is the exciton lifetime parameter (0.5 ns), r_F is the Förster radius (4.3 nm), r_{ij} is the distance from the initial chromophore to the hop destination, and B is a coefficient that takes into account the Boltzmann energy penalty for hopping upstream in energy ($\exp^{-\Delta E_{ij}/k_B T}$ for $\Delta E_{ij} > 0$, and 1 for $\Delta E_{ij} \leq 0$), as well as a variable prefactor that will be discussed later.

- If an exciton hops to a chromophore that is within 1 nm of an opposing chromophore type (i.e. both a donor and an acceptor chromophore in range), it will instantaneously dissociate (removed from the system) to create an electron on the acceptor chromophore and a hole on the donor.

- Excitons also are given a lifetime, t_{ex} based on τ_{ex} ($t_{\text{ex}} = -\ln(x\tau_{\text{ex}})$, where x is a random number in the interval $[0, 1)$). If the exciton would hop for any time longer than t_{ex}, it is instead removed from the system and counted as recombining, without generating charge carriers.

Note that all subsequent data has been run using the same random number seed to ensure comparable statistics.

2.1 Prefactor $= 1 \times 10^0$

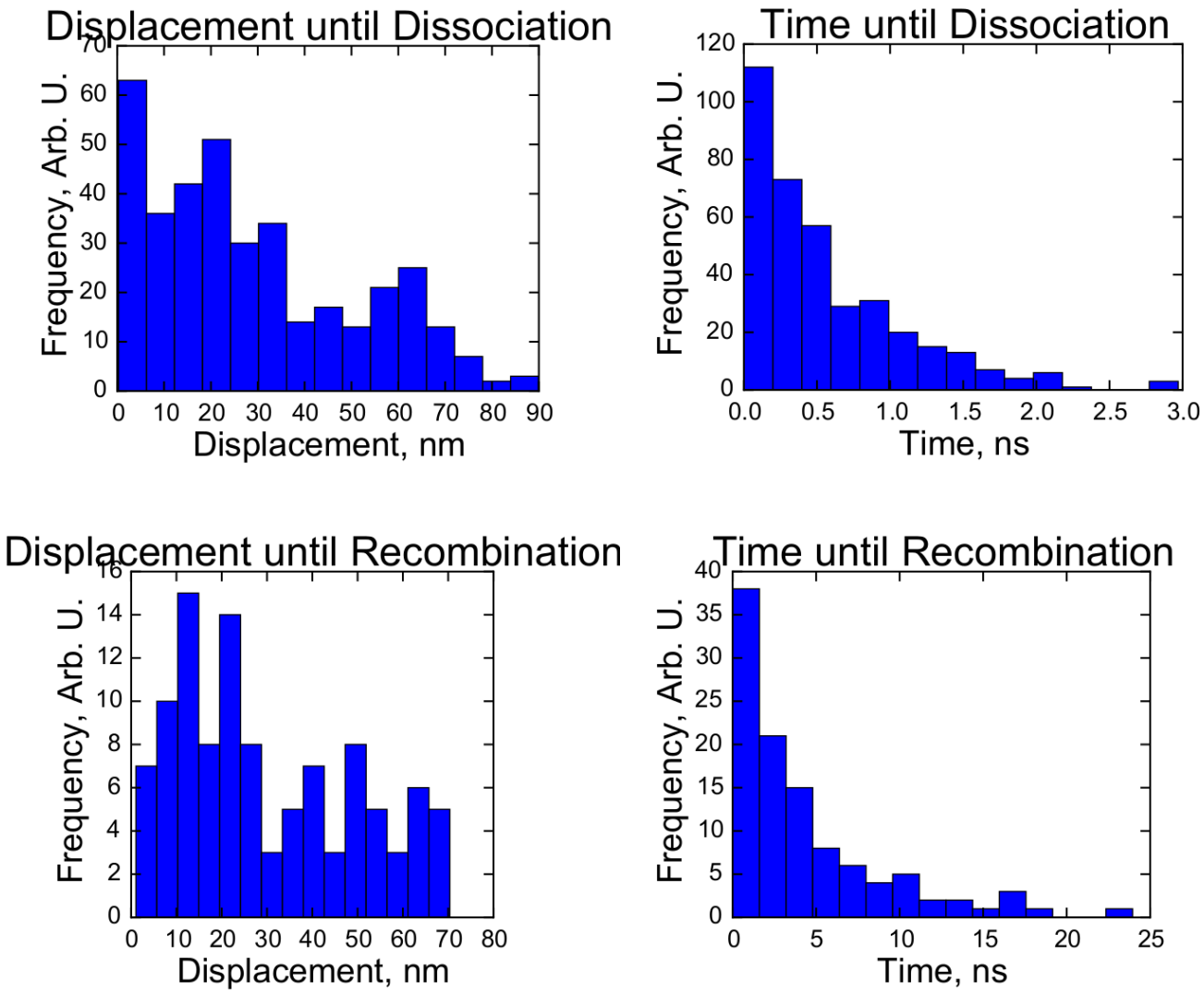

Figure 2: The measured exciton dynamics given a k_{FRET} prefactor of 1.0

- The above results incentivised the k_{FRET} equation modification as it seems to be unsuitable for describing this high-resolution exciton transport.
- Excitons are consistenly moving for many tens of nm, which is too high for this kind of organic system (somewhat based on P3HT:PCBM, which has a mean-free path length of around 5 nm.
- Additionally, the lifetimes of the non-dissociating excitons are far too high. The lifetime parameter should be restricting the lifetime to around 0.5 ns, not 20+.

- The driving factor in the equation is the $(\frac{r_F}{r_{ij}})^6$. r_{ij} is of the order angstroems, which forces the rate coefficient to be extremely high, allowing the exciton to move very far in a short space of time.
- As such, it might be a good idea to reduce the rate coefficient through the use of a prefactor, in order to get the expected exciton dynamics
- There is some partial justification in this according to Ref[1], which suggests that the intrinsic point-dipole assumption in FRET might not be suitable for some materials.
- This is a complicated issue though because Refs[1,2] also show diffusion lengths of around 40nm given 90 meV of energetic disorder and a Förster length of 4.3 nm, which isn't miles off.
- With a prefactor of 1.0, the exciton dissociation efficiency was 79% for our bilayer morphology.

2.2 Prefactor $= 1 \times 10^{-2}$

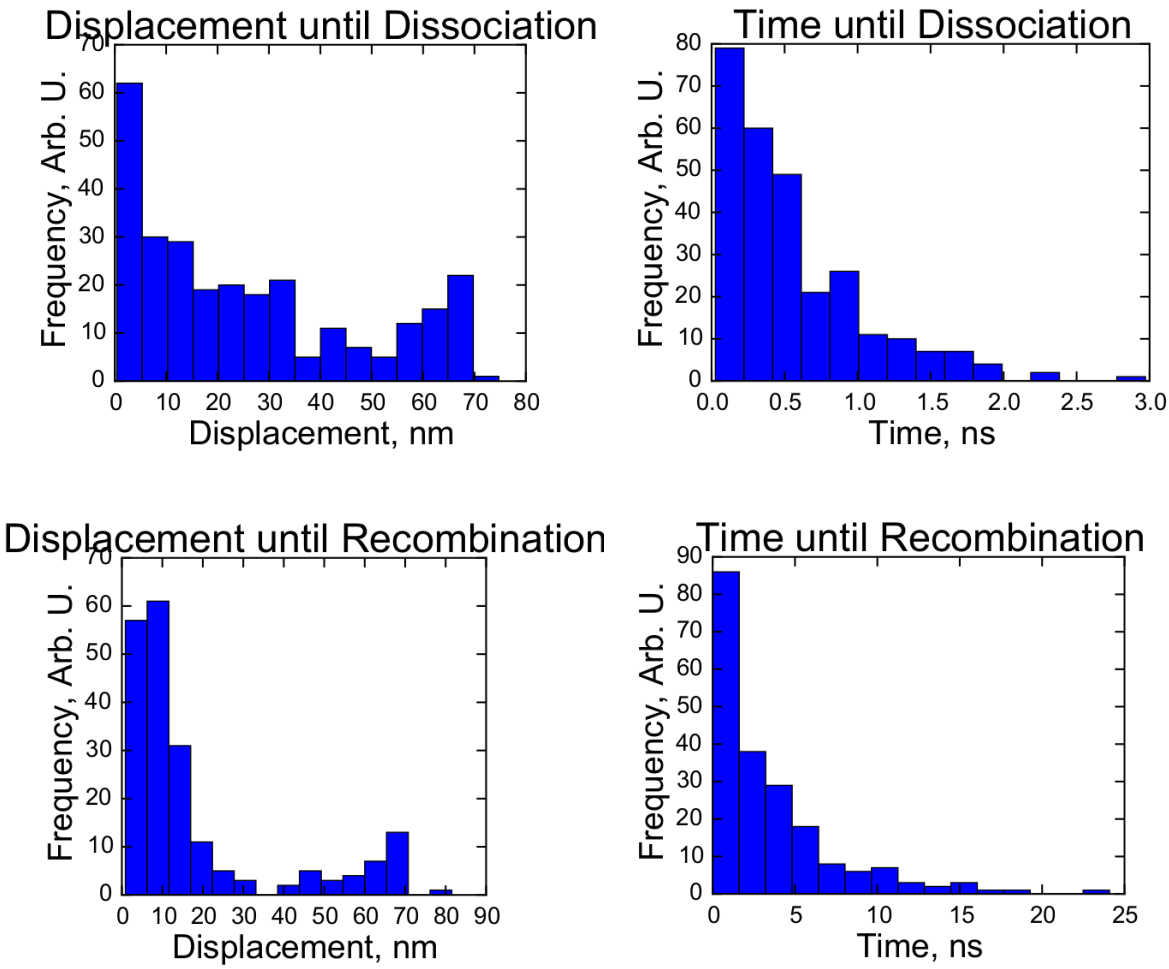

Figure 3: The measured exciton dynamics given a k_{FRET} prefactor of 0.01

- Reducing the FRET hopping rates by 2 orders of magnitude has improved the exciton dynamics slightly, as excitons travel less far before recombining. Around twice as many excitons are recombining within 0.5 ns, and the majority have a pre-recombination free path of less then 40 nm.
- With a prefactor of 0.01, the exciton dissociation efficiency was XX% for our bilayer morphology.

2.3 Prefactor $= 1 \times 10^{-4}$

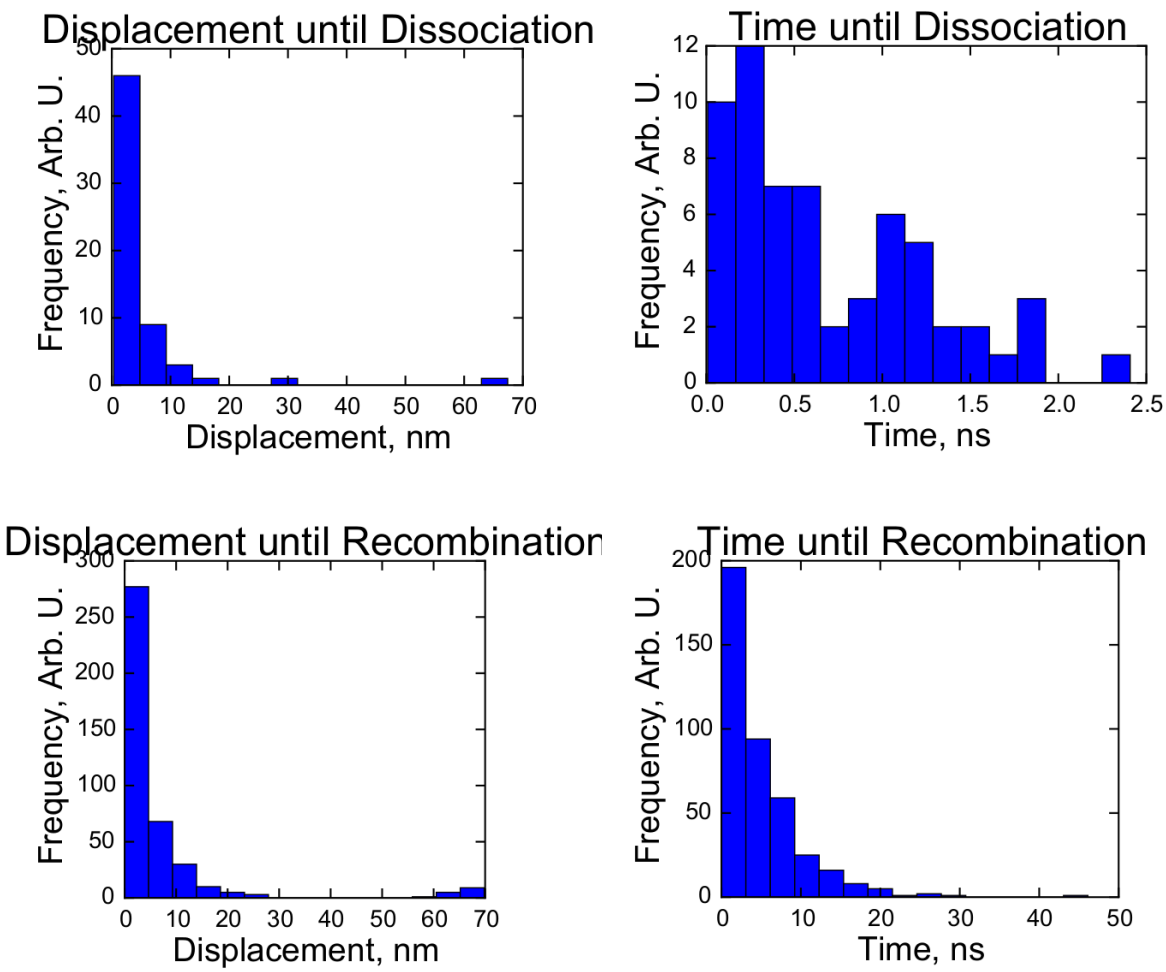

Figure 4: The measured exciton dynamics given a k_{FRET} prefactor of 0.0001

- Reducing the FRET hopping rates to 1×10^{-4} has affected the exciton dynamics more strongly, with nearly all excitons dissociating or recombining within 30 nm (except for a small few that are spawned in crystals and so can travel significantly further) and a few nanoseconds.
- With a prefactor of 1×10^{-4}, the exciton dissociation efficiency was 12.6% for our bilayer morphology.

2.4 Summary of Prefactor Investigation

Prefactor	Recombination		Dissociation		XDE
	Time (ns)	Disp (nm)	Time (ns)	Disp (nm)	%
1×10^{0}	0.45 ± 0.04	30 ± 2	0.57 ± 0.03	29 ± 1	77.8
1×10^{-2}	0.35 ± 0.03	18 ± 1	0.55 ± 0.03	26 ± 1	58.2
1×10^{-4}	0.48 ± 0.03	6.3 ± 0.6	0.69 ± 0.07	5 ± 1	12.6

Table 2: The morphologies selected for use in each cell in the device. The ID integers correspond to 'moietyType', and '$l_{x,y,z}$' is the cubic box length for each molecular system.

- Modifying the prefactor does not significantly affect the average recombination or dissociation time, however, it does strongly affect the distance that the exciton can travel.
- Additionally, it significantly reduces simulation runtime, which will be important during the full carrier-included device simulations as exciton transport is not expected to be the most computationally intensive part of the simulation.
- In order to obtain the 'correct' [CITATION NEEDED] path lengths for excitons in the sorts of systems that we are investigating, we should modify the Förster transport rate by a prefactor of 1×10^{-4} to ensure consistent exciton dynamics.

3 Carrier Hopping ΔE

The ΔE in the Marcus hopping equation is quite different for device-scale simulations.

The following components are required:

- The chromophore energy difference that was used previously (ΔE_{ij} - note that this is 0 for small molcules, so it might be important to add some energetic disorder to this if we deem it necessary)
- The drift component. Now that we're simulating a full device, there is a potential within the system that biases hops along the z-axis due to the potential applied across the electrical contacts. As the field increases, electrons are forced through the anode, which reduces the number of extractions and therefore the ouput current of the device. Holes are forced in the opposite direction.
- Finally, since we are now simulating more than one charge carrier, the Coulombic effects of nearby carriers must be taken into account. The Durham code also includes image charges, and I've put in the infrastructure for this, but I don't really understand their prescence properly, so I'm trying without them for now to see what we get. I'll dig into Ben and Chris' old papers to learn more about these images.

These components will probably need a lot more testing, but preliminary data shows the following magnitudes for these components:

- The ΔE_{ij} component has a magnitude of several hundred meV, unless we're dealing with hopping between small molecules (i.e. identical chromophores) in which case $\Delta E_{ij} = 0$.
- The drift component is pretty small. In the case of an applied voltage of 0.2 (corresponding to a field of around 1×10^7 Vm^{-1}), the component contribues ~ 1 meV to the ΔE. This could be on the small side, or it could be exactly right - I just don't know. One thing I can do is take a look at the Durham data (on my laptop) to see if we ever output those magnitudes anywhere that might be able to give me some idea of if this is correct or not.
- The Coulombic effects have a magnitude of several hundred meV (for immediately dissociated carriers), and it feels sensible that the Coulomb potential is of similar order to the energetic disorder arising from chromophore fluctuations.

4 KMC Timescales

- A Fermi-estimate of the timescales involved in the KMC indicated that the carrier hops in P3HT (tons of single-monomer chromophores that are super close together) suggested that we were spanning ~ 16 orders of magnitude in time between our fastest and slowest events, from 1×10^{-18} s for the fastest carrier hops and 1×10^{-2} s for the photoinjections.
- Perhaps we can use the FRET hopping prefactor here to slow down the carrier hops as well, given that we justify the prefactor due to the tiny hops that occur between the densely packed chromophores. Using this prefactor slows down the mobilities that we obtained using the molecular KMC. The advantage is that this saves 4 orders of magnitude, bringing the difference down to 12.
- The incident flux was set to 0.01 mW/cm^2 rather than the 100 mW/cm^2 that correctly corresponds to AM1.5. This reduces the number of orders of magnitude by another 4 to 8.

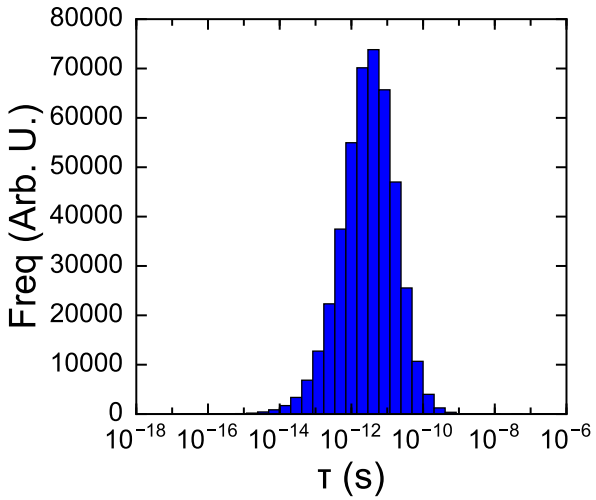

Figure 5: The distribution of the event timescales observed in a device simulation consisting of around 500,000 KMC iterations (corresponding to 23 photoinjections)

- Figure 5 shows the resultant distribution of timescales in the device simulations, after about 500,000 iterations ($\sim$ 15 minutes of runtime).
- The following data can be obtained from the distribution:
  - Slowest Event $= 5.00 \times 10^{-6}$ s
  - Fastest Event $= 1.21 \times 10^{-17}$ s
  - Mean $= 5.40 \times 10^{-11}$ s
  - STD $= 1.04 \times 10^{-8}$ s
- The results show a computationally tangible distribution of event times. While the range is still 11 orders of magnitude, the vast majority of events occur between 10^{-13} and 10^{-10} s.

Over the Freedom Day holiday, I ran a long simulation on my desktop to push the code to its limit and check for any more edge-cases that I might have missed. Here are the results of that investigation:

- Simulation Run-time:
  - Number of KMC Iterations: 47,994,911
  - Total Simulation Time: 4.58×10^{-4} s
  - Total Wall-Clock Time: 23 hours 11 minutes 34 seconds
- Simulation Events:
  - Excitons:
    - Total Number of Photoinjections: 501
    - Total Number of Exciton Dissociations: 89
    - Total Number of Exciton Recombinations: 412
    - Exciton Dissociation Efficiency: 17.8%
  - Carriers:
    - Total Number of Dark Injections: 0
    - Total Number of Carrier Extractions: 0
    - Total Number of Carrier Recombinations: 50
    - Carrier Separation Efficiency: 43.8%

No dark current injections occuring is weird, and further analysis has shown that I have my injection barriers the wrong way round. I am addressing this issue currently and will have new results available shortly.

5 Charge Carrier Trajectories

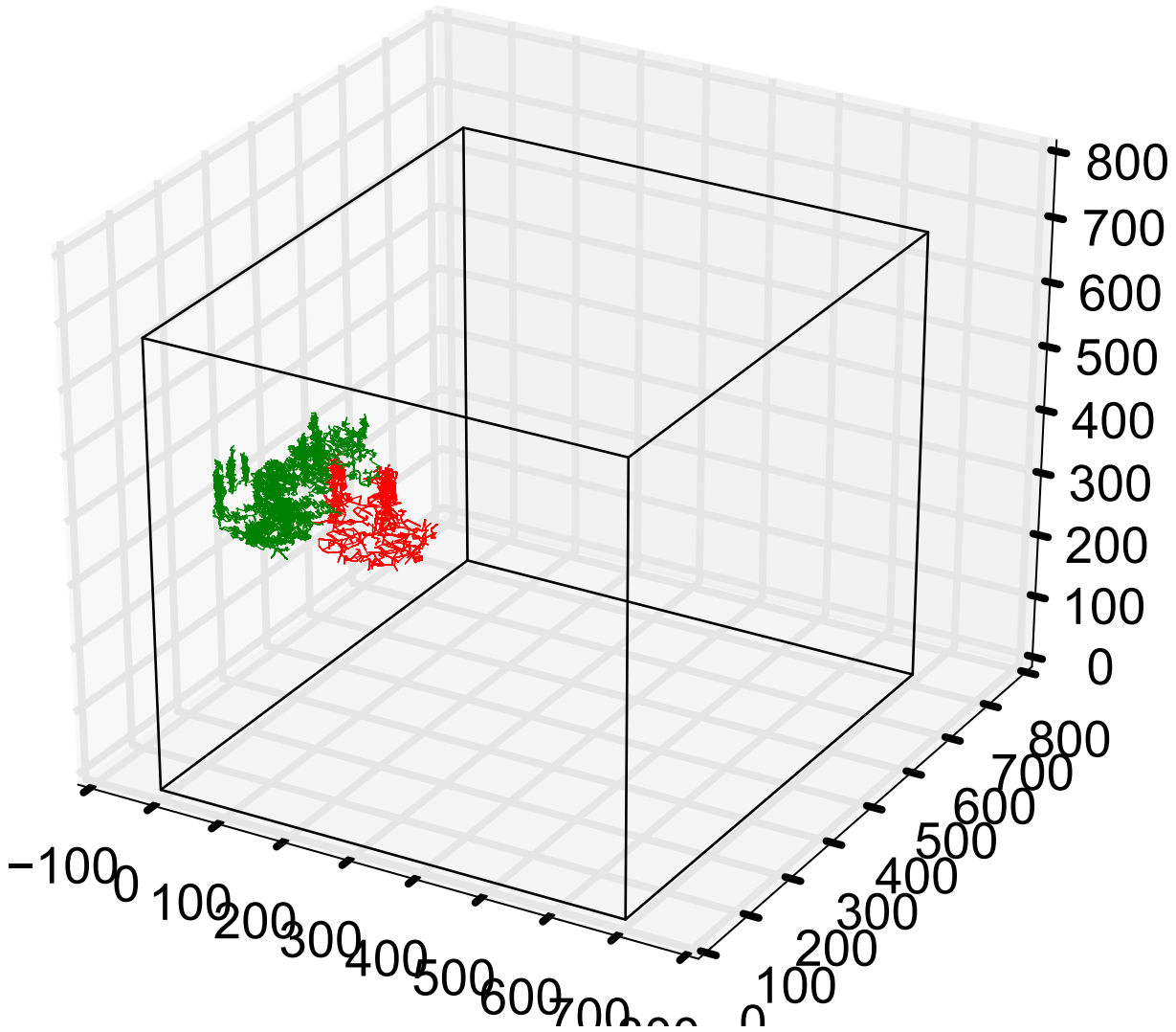

Figure 6: The trajectories of two charge carriers in a simulation of 4000 iterations, tracked from exciton dissocation. The red carrier is the electron, and the green carrier is the hole

- Check this out - you can tell that the green carrier is the hole because on the left hand side you can see that it enters into an ordered domain where it hopped up and down the z axis through the layers for a bit before entering another disordered cell nearby.

6 Dark Current Injection

The issues with the dark current injection were significantly harder and deeper than I anticipated.

6.1 Electrodes Upside Down

At the highest level, I had my electrodes upside down, such that the cathode was trying to inject holes and the anode was trying to inject electrons - neither of which could occur in the simulations because of the bilayer morphology. Flipping the contacts around led to issues with incredibly fast injection occuring, leading to a saturation of the top and bottom layers of the device and populating the queues with insanely long hop times (1×10^{99} s) because of the ridiculous Coulombic landscape near the interface.

6.2 Injection Rates Too Fast

1. Firstly I tried increasing the injection barrier, but that just prolonged the time until the saturation occured and the simulation crashed.

2. After thinking about it some more, I became convinced that Marcus hopping is not appropriate for carrier injection. What is the reorganisation energy of the electrode? What about the transfer integral between the electrode and the chromophore?

3. Instead I tried a simplified Miller Abrahams hopping equation, with a manually specified prefactor, and a simple distance calculation from the electrode to the injection site.

4. The prefactor was calibrated to give a sensible injection rate distribution in the event times within the 5-6 orders of magnitude of time that we can explore using this methodology.

5. This appeared to reconcile some of the problems, but the output J-V curves were still messy and slow.

Work on this morphology has been suspended indefinitely. Instead, I will be using a less complex system (called testSimple) containing just one moiety of donor and acceptor material rather than two each. The device is 3x3x3 instead of 9x9x9, and each moiety is the same size (10 nm). Additionally, the more computationally intensive calculations have been vectorised to try and speed up the calculations and reduce total simulation wall-clock time. Please see the 'SimpleDeviceKMC' summary for more details.

References

[1] Krishna Feron, Warwick Belcher, Christopher Fell, and Paul Dastoor. Organic Solar Cells: Understanding the Role of Förster Resonance Energy Transfer. *International Journal of Molecular Sciences*, 13(12):17019–17047, dec 2012.

[2] Stavros Athanasopoulos, Evguenia V. Emelianova, Alison B. Walker, and David Beljonne. Exciton diffusion in energetically disordered organic materials. *Physical Review B*, 80(19):195209, 2009.